Induction of prostaglandin E2 pathway promotes gastric hamartoma development with suppression of bone morphogenetic protein signaling.

Induction of prostaglandin E_2 pathway promotes gastric hamartoma development with suppression of bone morphogenetic protein signaling

Hiroko Oshima[1], Hiraku Itadani[2], Hidehito Kotani[2], Makoto Mark Taketo[3], and Masanobu Oshima[1]

[1]Division of Genetics, Cancer Research Institute, Kanazawa University, Japan; [2]Oncology Department, Banyu Tsukuba Research Institute, Japan; [3]Department of Pharmacology, Kyoto University Graduate School of Medicine, Japan

Corresponding author: Masanobu Oshima, Division of Genetics, Cancer Research Institute, Kanazawa University, 13-1 Takara-machi, Kanazawa 920-0934, Japan. Phone:+81-76-265-2721; FAX:+81-76-234-4519; E-mail, oshimam@kenroku.kanazawa-u.ac.jp

Running Title: Gastric hamartoma by BMP suppression and PGE_2 induction

Key words: gastric hamartoma, BMP, PGE_2, COX-2, juvenile polyposis

Abstract

Mutations in bone morphogenetic protein (BMP) receptor 1A (*BMPR1A*) are responsible for a subset of cases of juvenile polyposis (JP) syndrome that develops hamartomatous tumors in the gastrointestinal tract. Mouse genetic studies have demonstrated that suppression of BMP signaling in the intestines causes JP-type hamartoma development. Here, we generated *K19-Nog* transgenic mice expressing noggin, a BMP antagonist, in gastric epithelium. However, inhibition of BMP signaling did not cause gastric phenotypes. We thus crossed *K19-Nog* with *K19-C2mE* mice that expressed *Ptgs2* and *Ptges* in the stomach to generate compound transgenic mice. Expression of *Ptgs2* and *Ptges* results in prostaglandin E_2 (PGE_2) biosynthesis, and both enzymes are induced in most human gastrointestinal tumors. Importantly, *K19-Nog/C2mE* compound mice developed gastric hamartomas that were morphologically similar to those found in JP with mucin-containing dilated cysts and inflammatory infiltration. Notably, treatment of *K19-Nog/C2mE* mice with a COX-2 inhibitor, celecoxib, significantly reduced tumor size with suppression of angiogenesis, suggesting that induction of the PGE_2 pathway together with inhibition of BMP signaling is required for gastric hamartoma development. Moreover, microarray analyses revealed that canonical Wnt signaling target genes were not induced in *K19-Nog/C2mE* hamartomas, indicating that BMP inhibition and PGE_2 induction lead to gastric hamartoma development independent of the Wnt/β-catenin pathway. These results, taken together, suggest that the PGE_2 pathway is an effective preventive target against BMP-suppressed gastric

hamartomas, as well as for Wnt/β-catenin-activated adenocarcinomas.

Introduction

Juvenile polyposis (JP) is a hereditary gastrointestinal hamartomatous polyposis syndrome (1). Germline mutations in bone morphogenetic protein (BMP) receptor type IA gene (*BMPR1A*) have been found in a subpopulation of JP patients (2). BMP ligands bind to a complex of the BMP receptor type II and type I, which leads to phosphorylation of Smad1,5,8, allowing them to form a complex with Smad4 (3, 4). These Smad complexes translocate to nuclei and function as transcription enhancers. BMP signaling inhibits epithelial cell proliferation and promotes differentiation (5, 6), and suppression of BMP signaling in mice results in intestinal hamartomatous polyp development through activation of the PI3K-Akt pathway (6, 7). Moreover, intestinal epithelial cell-specific deletion of *Bmpr1a* results in elongated villi and crypt fission (8). These results indicate that BMP signaling promotes intestinal epithelial differentiation, and thus suppression of the BMP pathway causes tumorigenesis. Although the main affected site of tumors in JP patients is the colon, gastric polyps have been found in 14% of JP patients, and cancer risk in JP patients increases both in the colon and stomach (9, 10). Recently, it was reported that disruption of *Bmpr1a* in mouse stomach results in development of tumorous lesions in squamocolumnar and gastrointestinal transition zones, suggesting that suppression of BMP signaling triggers tumor development also in the stomach (11).

On the other hand, we found that expression of cyclooxigenase-2 (COX-2) and microsomal prostaglandin E synthase-1 (mPGES-1) is induced simultaneously in

gastrointestinal tumor tissues (12). COX-2 and mPGES-1 are functionally coupled for biosynthesis of prostaglandin E_2 (PGE_2) (13) that plays a critical role in tumorigenesis in the gastrointestinal tract (14-17). However, the role of the PGE_2 pathway in hamartomatous tumors is not understood. We constructed transgenic mice expressing *Nog* encoding noggin in the gastric mucosa and crossed them with another transgenic mice expressing both *Ptgs2* and *Ptges* encoding COX-2 and mPGES-1, respectively, (16). We show that inhibition of BMP signaling is not sufficient for gastric tumorigenesis, but that BMP suppression together with PGE_2 induction causes development of JP-type gastric hamartoma.

Materials and Methods

Mouse models. *K19-C2mE* mice expressing *Ptgs2* and *Ptges*; *K19-Wnt1* mice expressing *Wnt1*; and *K19-Wnt1/C2mE* mice expressing *Wnt1, Ptgs2*, and *Ptges*, were described previously (16, 17). pK19-Nog was constructed using keratin 19 gene promoter, mouse *Nog* cDNA, and SV40 p(A) cassette (Fig. 1A). The expression vector was microinjected into the fertilized eggs of F1 (C3H and C57BL/6) mice (CLEA, Japan) to generate *K19-Nog* mice. Primer sequences used for genotyping: (F-5'-GTACGCGTGGAATGACCTAGG-3', F-5'-GCAAAGGGTCGCTACAGACGT-3'). Transgenic vector constructs are shown in Figure 1A. *K19-Nog* and *K19-C2mE* mice were crossed to generate *K19-Nog/C2mE* mice. Gastric phenotypes of these mice were examined at 30 weeks of age. For inhibition of COX-2, mice were administered *p.o.* with celecoxib (Pfizer) at 100 mg/kg/day for 3 weeks. All animal experiments were carried out according to the protocol approved by Ethics Committees on Animal Experimentation of Kanazawa University.

Real-time RT-PCR. Total RNA was reverse-transcribed and PCR-amplified. Primer sets used in real-time RT-PCR for detection of *Nog, Ptgs2, Ptger1, Ptger2, Ptger3* and *Ptger4* were purchased (TakaraBio, Japan).

Histology. Tissues were fixed in 4% paraformaldehyde, paraffin-embedded, and sectioned at 4-μm thickness. The following antibodies were used for immunostaining: anti-COX-2 (Cayman Chemical), anti-F4/80 (Serotec, Oxford, UK), anti-α-smooth muscle actin (α-SMA) (Sigma), anti-Ki-67, anti-von Willebrand factor

(DakoCytomation), and anti-phosphorylated Smad1,5,8 (Chemicon). Staining signal was visualized using the Vectorstain Elite Kit (Vector Laboratories).

X-ray CT. *K19-Nog/C2mE* mice were subjected to X-ray CT using LaTheta LCT-100 (Aloka, Japan). CT analyses were performed 1 week before celecoxib treatment and at 0, 1, 2 and 3 weeks after treatment. Tumor size on CT images was measured using NIH Image software (NIH).

Immunoblotting. Tissue samples were homogenized in lysis buffer. Protein samples were separated in a SDS-polyacrylamide gel. Antibody for the active β-catenin (Upstate) was used. The ECL detection system (Amersham) was used to detect specific signals.

Microarray analyses. Total RNA were prepared from mouse stomach at 30 weeks of age. Expression profiles of the Wnt target genes (http://www.stanford.edu/~rnusse/wntwindow.html), cytokines, and chemokines were examined with the Affymetrix GeneChip system and Mouse Genome 430 2.0 Arrays (Affymetrix).

Statistical analyses. Statistical analyses were carried out using Student's *t*-test.

Results and Discussion

Generation of *K19-Nog* transgenic mice. To suppress BMP signaling in the stomach, we constructed *K19-Nog* mice that expressed *Nog* encoding noggin in gastric epithelial cells (Fig. 1A). Noggin is a polypeptide that inhibits BMP signaling by binding BMP ligands (4). We confirmed increased levels of *Nog* mRNA in *K19-Nog* mouse stomach compared with that in the wild-type by real-time RT-PCR (Fig. 1B). BMP type I receptor phosphorylates Smad1,5,8 upon complex formation with BMP ligand and type II receptor (3). We found phosphorylated Smad1,5,8 by immunohistochemistry in the nuclei of differentiated epithelial cells both at the surface and bottom of the gastric gland (Fig. 1C), which is consistent with a previous report (11). Notably, in the *K19-Nog* mice, the immunostaining signals of phosphorylated Smad1,5,8 decreased significantly in the upper gastric gland where the K19 promoter is transcriptionally active (Fig. 1C, D). These results indicate that exogenous *Nog* expression inhibits BMP signaling in the stomach.

Construction of compound mutant mice. We previously constructed *K19-C2mE* transgenic mice expressing both *Ptgs2* and *Ptges* encoding COX-2 and mPGES-1, respectively, in gastric mucosa (Fig. 1A, D). Expression of COX-2 and mPGES-1 leads to increase of PGE_2 level in *K19-C2mE* mouse stomach (16). To investigate the effect of the PGE_2 pathway in BMP-suppressed gastric mucosa, we crossed *K19-Nog* and *K19-C2mE* mice to generate *K19-Nog/C2mE* compound mice. We confirmed expression of *Ptgs2* by real-time RT-PCR in the stomach of *K19-C2mE* and *K19-Nog/C2mE* mice, but not in wild-type and *K19-Nog* mice (Fig.

1B). We also used *K19-Wnt1/C2mE* mice for this study that develop gastric adenocarcinoma caused by simultaneous activation of the Wnt and PGE_2 pathways (17). Genotypes of respective transgenic strains were confirmed by genomic PCR (Supplementary Fig. 1).

Gastric tumor development in *K19-Nog/C2mE* mice. *K19-Nog* mice did not develop tumorous lesions in the stomach, and the histology of gastric glands was normal (Supplementary Fig. 2, and Fig. 2A). In contrast, *K19-C2mE* mice developed inflammation-associated hyperplasia, and *K19-Wnt1* mice developed dysplastic preneoplastic lesions, which were consistent with previous reports (16, 17). Importantly, *K19-Nog/C2mE* mice develop large tumors in the glandular stomach (Supplementary Fig. 2, and Fig. 2A). These results suggest that suppression of BMP signaling is insufficient for gastric tumorigenesis, but that cooperation of BMP inhibition and PGE_2 induction cause gastric tumor development. Such an effect of PGE_2 on tumorigenesis was similar to that found in *K19-Wnt1/C2mE* mice. Activation of Wnt/β-catenin alone leads to development of small preneoplastic lesions, whereas simultaneous activation of the Wnt/β-catenin and PGE_2 pathways cause gastric adenocarcinoma (17, and Fig. 2A). Therefore, PGE_2 plays an important role in tumorigenesis regardless of the types of genetic alterations.

JP-type hamartoma in *K19-Nog/C2mE* mouse stomach. Histologically, gastric tumors in *K19-Nog/C2mE* mice displayed irregular branching of epithelial cell layers, combined with dilated cysts that were filled with mucin (Fig. 2B and C). Such histological characteristics were different from dysplastic tumors of the

K19-Wnt1/C2mE mice (17, and Fig 2B). We also found abundant α-smooth muscle actin-positive myofibroblasts in stroma. Moreover, we detected infiltration of F4/80-positive macrophages and the accumulation of lymphocytes in the *K19-Nog/C2mE* tumors (Fig. 2C). These histological characteristics are typical of the hamartoma of JP patients (9, 10, 18), indicating that suppression of BMP signaling associated with PGE_2 induction causes development of JP-type gastric hamartoma. However, tumor incidence in *K19-Nog/C2mE* mice was 23%, whereas that in *K19-Wnt1/C2mE* mice was 100% (Supplementary Table). Notably, expression of inflammatory cytokine TNF-α increased in *K19-Nog/C2mE* hamartomas as well as in *K19-C2mE* hyperplasia (Supplementary Fig. S3). However, TNF-α was not induced in non-tumor stomach of *K19-Nog/C2mE* mice, while transgenic expression of *Ptgs2* stayed at the same level as that in tumor tissues. These results suggest that inflammatory response is also important for hamartoma development together with BMP suppression and PGE_2 induction.

Suppression of gastric hamartoma by COX-2 inhibition. To investigate whether the PGE_2 pathway is required for gastric hamartoma development, we treated *K19-Nog/C2mE* mice with a COX-2 selective inhibitor, celecoxib, at 100 mg/kg/day for 3 weeks. We examined gastric tumor size by X-ray CT scanning, and found that the tumor volume of *K19-Nog/C2mE* mice decreased significantly by celecoxib treatment (Fig. 3A). The mean relative tumor size on CT images reduced to 58% after celecoxib treatment (Fig 3B). Histologically, cystic structures were no longer found, and necrotic area was detected in the celecoxib-treated

K19-Nog/C2mE tumors (Fig. 3C). The PGE_2 pathway is important for angiogenesis of gastrointestinal tumorigenesis (15, 19). Consistently, the number of capillary vessels decreased significantly in celecoxib-treated *K19-Nog/C2mE* tumors (Fig. 3D). Accordingly, it is possible that angiogenesis is one of the important functions of PGE_2 for hamartoma development.

Wnt-independent development of gastric hamartoma. In the intestinal crypt, inhibition of BMP signaling results in activation of the Wnt/β-catenin pathway (7). We thus examined activation of Wnt signaling in *K19-Nog/C2mE* gastric tumors. The level of the active β-catenin did not increase in *K19-Nog/C2mE* hamartomas, while it elevated markedly in *K19-Wnt1/C2mE* tumors (Fig. 4A). Consistently, expression of Wnt target genes in *K19-Nog/C2mE* tumors stayed at the same level as that in wild-type mouse stomach, while these genes were upregulated in *K19-Wnt1/C2mE* tumors (Fig. 4B). We confirmed that inflammatory cytokines and chemokines were induced in both *K19-Nog/C2mE* and *K19-Wnt1/C2mE* tumors. Accordingly, activation of Wnt signaling is not involved in hamartoma development in BMP-suppressed gastric mucosa, although PGE_2 signaling or PGE_2-dependent inflammation may be required for both adenocarcinoma and hamartoma.

We next examined expression of PGE_2 receptors, EP1 to EP4 in tumor tissues. Notably, the expression of *Ptger1*, *Ptger2*, and *Ptger3* encoding EP1, EP2, and EP3, respectively, decreased significantly in tumors of *K19-Nog/C2mE* and *K19-Wnt1/C2mE* mice (Fig. 4C). In contrast, expression of *Ptger4* encoding EP4 increased dramatically in both *K19-Nog/C2mE* hamartomas and *K19-Wnt1/C2mE*

adenocarcinomas. These results suggest that PGE_2 signaling through EP4 is important for development of both gastric hamartoma and adenocarcinoma. Namely, it is possible that the type of genetic alterations determines the histological phenotype of tumors, hamartoma or adenocarcinoma, and that the induced PGE_2 pathway promotes tumor growth through EP4 receptor regardless of histological types (Supplementary Fig. S4).

In human stomach, expression of COX-2 is induced in *Helicobacter pylori*-associated gastric lesions (20). Accordingly, it is conceivable that *H. pylori* infection contributes to the development of gastric hamartoma through induction of the PGE_2 pathway. Therefore, inhibition of the PGE_2 pathway as well as eradication of *H. pylori* may be an effective preventive strategy not only for gastric cancer but also for gastric hamartoma.

Acknowledgments

Grant support: This study was supported by Grants-in-Aid from the Ministry of Education, Culture, Sports, Science and Technology of Japan, and from the Ministry of Health, Labour and Welfare of Japan.

We thank Manami Watanabe for excellent technical assistance.

References

1. Entius MM, Westerman AM, van Velthuysen ML, et al. Molecular and phenotypic markers of hamartomatous polyposis syndromes in the gastrointestinal tract. Hepatogastroenterology 1999;46:661-6.
2. Howe JR, Bair JL, Sayed MG, et al. Germline mutations of the gene encoding bone morphogenetic protein receptor 1A in juvenile polyposis. Nat Genet 2001;28:184-7.
3. Miyazono K, Maeda S, Imamura T. BMP receptor signaling: Transcriptional targets, regulation of signals, and signaling cross-talk. Cytokine Growth Factor Rev 2005;16:251-63.
4. Chen D, Zhao M, Mundy GR. Bone morphogenetic proteins. Growth Factors 2004;22:233-41.
5. Hardwick JCH, van den Brink GR, Bleuming SA, et al. Bone morphogenetic protein 2 is expressed by, and acts upon, mature epithelial cells in the colon. Gastroenterology 2004;126:111-21.
6. Haramis A-PG, Begthel H, van den Born M, et al. Be novo crypt formation and juvenile polyposis on BMP inhibition in mouse intestine. Science 2004;303:1684-6.
7. He XC, Zhang J, Tong W-G, et al. BMP signaling inhibits intestinal stem cell self-renewal through suppression of Wnt-β-catenin signaling. Nat Genet 2004;36:1117-21.
8. Auclair BA, Benoit YD, Rivard N, Mishina Y, Perreault N. Bone morphogenetic

protein signaling is essential for terminal differentiation of the intestinal secretory cell lineage. Gastroenterology 2007;133:887-96.

9. Chow E, Macrae F. Review of juvenile polyposis syndrome. J Gastroenterol Hepatol. 2005;20:1634-40.

10. Schreibman IR, Baker M, Amos C, McGarrity TJ. The hamartomatous polyposis syndromes: A clinical and molecular review. Am J Gastroenterol 2005;100:476-90.

11. Bleuming SA, He XC, Kodach LL, et al. Bone morphogenetic protein signaling suppresses tumorigenesis at gastric epithelial transition zone in mice. Cancer Res 2007;67:8149-55.

12. Takeda H, Miyoshi H, Tamai Y, Oshima M, Taketo MM. Simultaneous expression of COX-2 and mPGES-1 in mouse gastrointestinal hamartomas. Br J Cancer 2004;90:701-4.

13. Murakami M, Naraba H, Tanioka T, et al. Regulation of prostaglandin E_2 biosynthesis by inducible membrane-associated prostaglandin E_2 synthase that acts in concert with cyclooxygenase-2. J Biol Chem 2000;275:32783-92.

14. Oshima M, Dinchuk JE, Kargman SL, et al. Suppression of intestinal polyposis in *Apc*$^{\Delta 716}$ knockout mice by inhibition of cyclooxygenase 2 (COX-2). Cell 1996;87:803-9.

15. Sonoshita M, Takaku K, Sasaki N, et al. Acceleration of intestinal polyposis through prostaglandin receptor EP2 in *Apc*$^{\Delta 716}$ knockout mice. Nat Med 2001;7:1048-51.

16. Oshima H, Oshima M, Inaba K, Taketo MM. Hyperplastic gastric tumors induced by activated macrophages in COX-2/mPGES-1 transgenic mice. EMBO J 2004;23:1669-78.

17. Oshima H, Matsunaga A, Fujimura T, Tsukamoto T, Taketo MM, Oshima M. Carcinogenesis in mouse stomach by simultaneous activation of the Wnt signaling and prostaglandin E_2 pathway. Gastroenterology 2006;131:1086-95.

18. Covarrubias DJ, Huprich JE. Best cases from the AFIP. Juvenile polyposis of the stomach. Radiographics 2002;22:415-20.

19. Guo X, Oshima H, Taketo MM, Oshima M. Stromal fiboblasts activated by tumor cells promote angiogenesis in mouse gastric cancer. J Biol Chem 2008;283:19864-71.

20. Sung JJY, Leung WK, Go MYY, et al. Cyclooxygenase-2 expression in *Helicobacter pylori*-associated premalignant and malignant gastric lesions. Am J Pathol 2000;157:729-35.

Figure Legends

Figure 1. Generation of transgenic mice. *A*, transgenic vectors. *B*, relative mRNA levels (Mean ± S.D.) of *Nog* and *Ptgs2* in the gastric mucosa of *K19-Nog* (*Nog*), *K19-C2mE* (*C2mE*), and *K19-Nog/C2mE* (*Nog/C2mE*) mice to the wild-type (*WT*). Asterisks, $p < 0.05$. *C*, immunohistochemistry of phosphorylated Smad1,5,8 in gastric mucosa of wild-type and *K19-Nog* mice. Arrowheads and arrows indicate positive nuclear staining in surface and gland bottom, respectively. Asterisks indicate decreased immunostaining signal in *K19-Nog* mouse. *D*, immunohistochemistry of COX-2 in wild-type and *K19-C2mE* mouse stomach. Arrows indicate transgenic expression of COX-2 in *K19-C2mE* gastric mucosa where *K19* promoter is transcriptionally active. *Bars*, 100 μm.

Figure 2. Gastric tumors developed in *K19-Nog/C2mE* mice. *A*, macroscopic photographs and H&E of *K19-Nog*, *K19-C2mE*, and *K19-Wnt1* mouse stomach (*top*). Arrowheads and asterisks in *K19-C2mE* indicate hyperplasia, and arrows indicate inflammatory infiltration. Arrowhead and inset in *K19-Wnt1* indicate preneoplastic lesion. Gastric tumors in *K19-Nog/C2mE* and *K19-Wnt1/C2mE* mice are shown (*arrows*, *bottom*). *Bars*, 10 mm. *B.* Histology of gastric tumors of *K19-Nog/C2mE* and *K19-Wnt1/C2mE* (H&E). *Bars*, 200 μm. *C*, PAS-Alcian blue, immunostaining for αSMA, F4/80, and H&E of *K19-Nog/C2mE* hamartomas (from *left* to *right*). Asterisks indicate dilated cysts. Arrows indicate lymphocyte accumulation. *Bars*, 100 μm.

Figure 3. Suppression of hamartoma development by COX-2 inhibition. *A*, X-ray CT images of gastric tumors of the same *K19-Nog/C2mE* mouse (*yellow dashed lines*) at 0 and 3 weeks of celecoxib treatment. *B*, relative tumor size at each time point of celecoxib treatment to the level at 0 week (Mean ± S.D.). *C*, representative photograph and H&E of celecoxib-treated *K19-Nog/C2mE* tumors. Arrow and asterisk indicate necrotic area. *D*, immunostaining for vWF. Arrows indicate vWF-positive capillary vessels. Microvessel densities (*MVD*) are shown (Mean ± S.D.). Asterisks, $p < 0.05$.

Figure 4. Wnt activity and EP expression in gastric hamartomas. *A*, Western blotting for active β-catenin in the stomach of each genotype. *B*, relative expression levels determined by microarray analyses of Wnt target genes and cytokines/chemokines in *K19-Wnt1/C2mE* and *K19-Nog/C2mE* tumors to the wild-type level. *C*, relative expression levels of PGE_2 receptors, *Ptger1, Ptger2, Ptger3*, and *Ptger4* in *K19-C2mE* hyperplasia, *K19-Nog/C2mE* hamartoma, and *K19-Wnt1/C2mE* adenocarcinoma (Mean ± S.D.). Asterisks, $p < 0.05$.

Figure 1

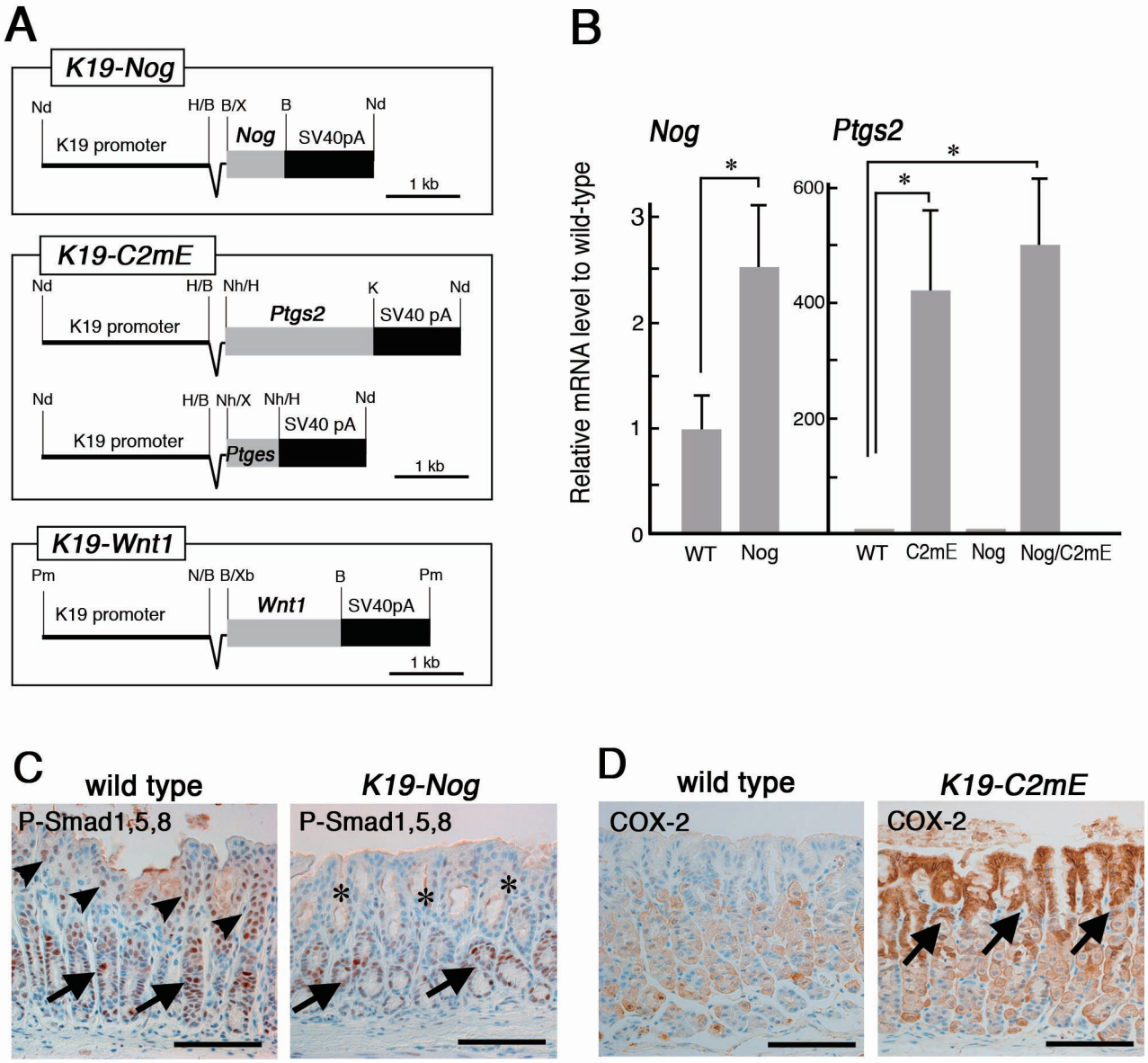
A
K19-Nog
Nd
H/B B/X
B
Nd
K19 promoter
Nog
SV40pA
1 kb
K19-C2mE
Nd
H/B Nh/H
K
Nd
K19 promoter
Ptgs2
SV40 pA
Nd
H/B Nh/X Nh/H
Nd
K19 promoter
SV40 pA
Ptges
1 kb
K19-Wnt1
Pm
N/B B/Xb
B
Pm
K19 promoter
Wnt1
SV40pA
1 kb
B
Nog
Ptgs2
Relative mRNA level to wild-type
0
1
2
3
200
400
600
*
*
*
WT
Nog
WT
C2mE
Nog
Nog/C2mE
C
wild type
K19-Nog
P-Smad1,5,8
P-Smad1,5,8
D
wild type
K19-C2mE
COX-2
COX-2

Figure 2

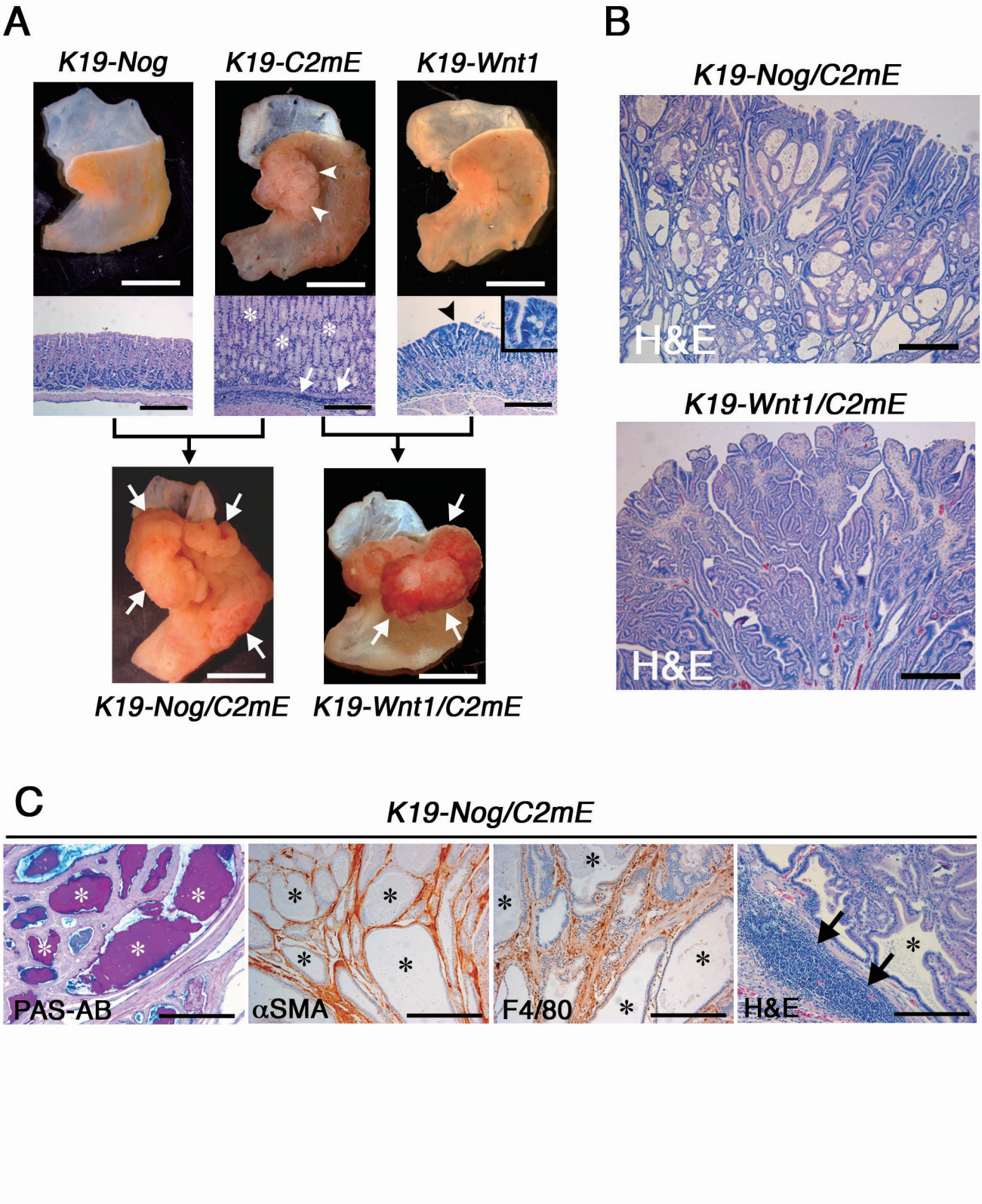
A
K19-Nog
K19-C2mE
K19-Wnt1
K19-Nog/C2mE
K19-Wnt1/C2mE
B
K19-Nog/C2mE
H&E
K19-Wnt1/C2mE
H&E
C
K19-Nog/C2mE
PAS-AB
αSMA
F4/80
H&E

Figure 3

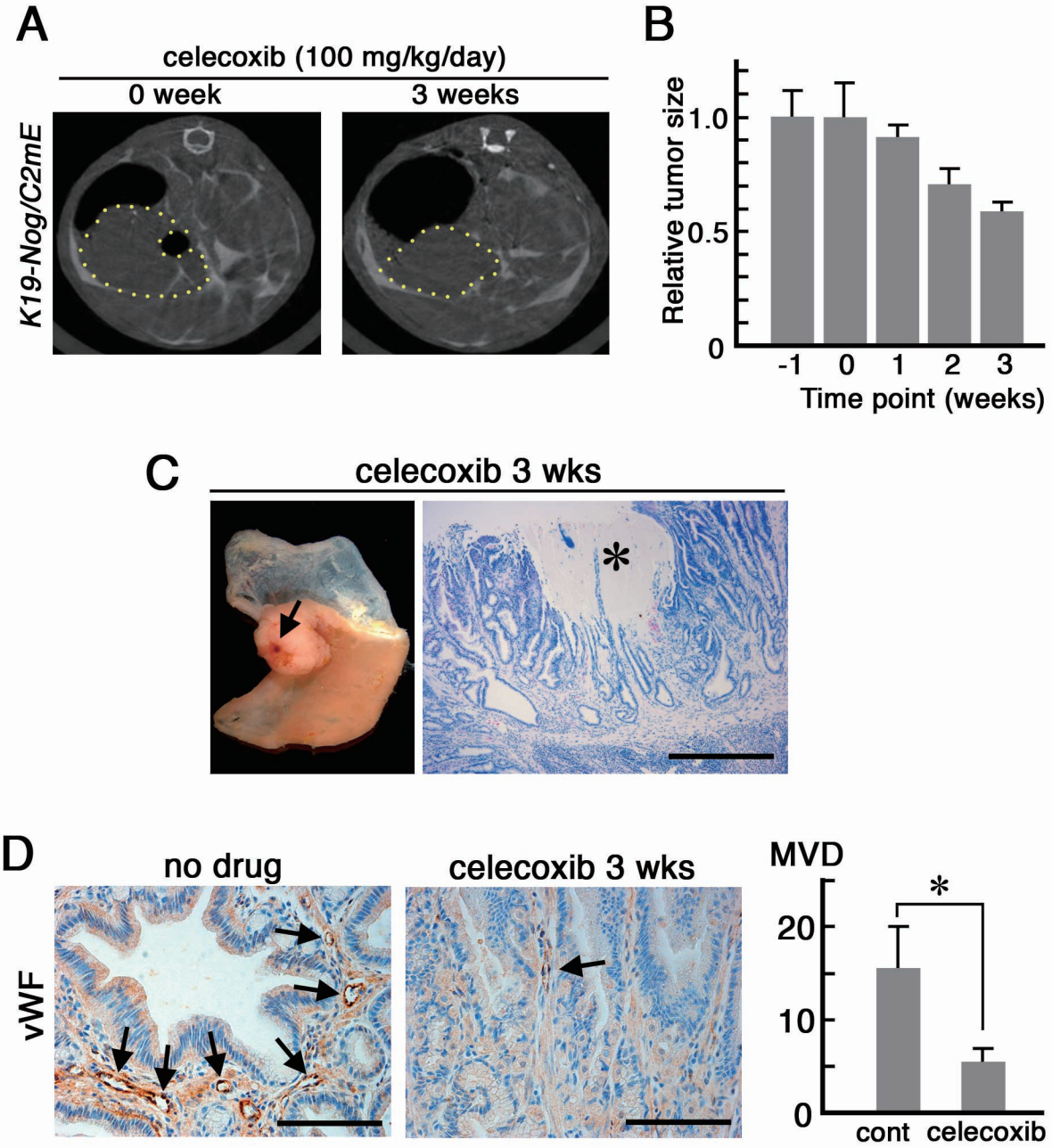
A
celecoxib (100 mg/kg/day)
0 week
3 weeks
K19-Nog/C2mE
B
Relative tumor size
1.0
0.5
0
-1
0
1
2
3
Time point (weeks)
C
celecoxib 3 wks
*
D
no drug
celecoxib 3 wks
vWF
MVD
*
20
10
0
cont
celecoxib

Figure 4

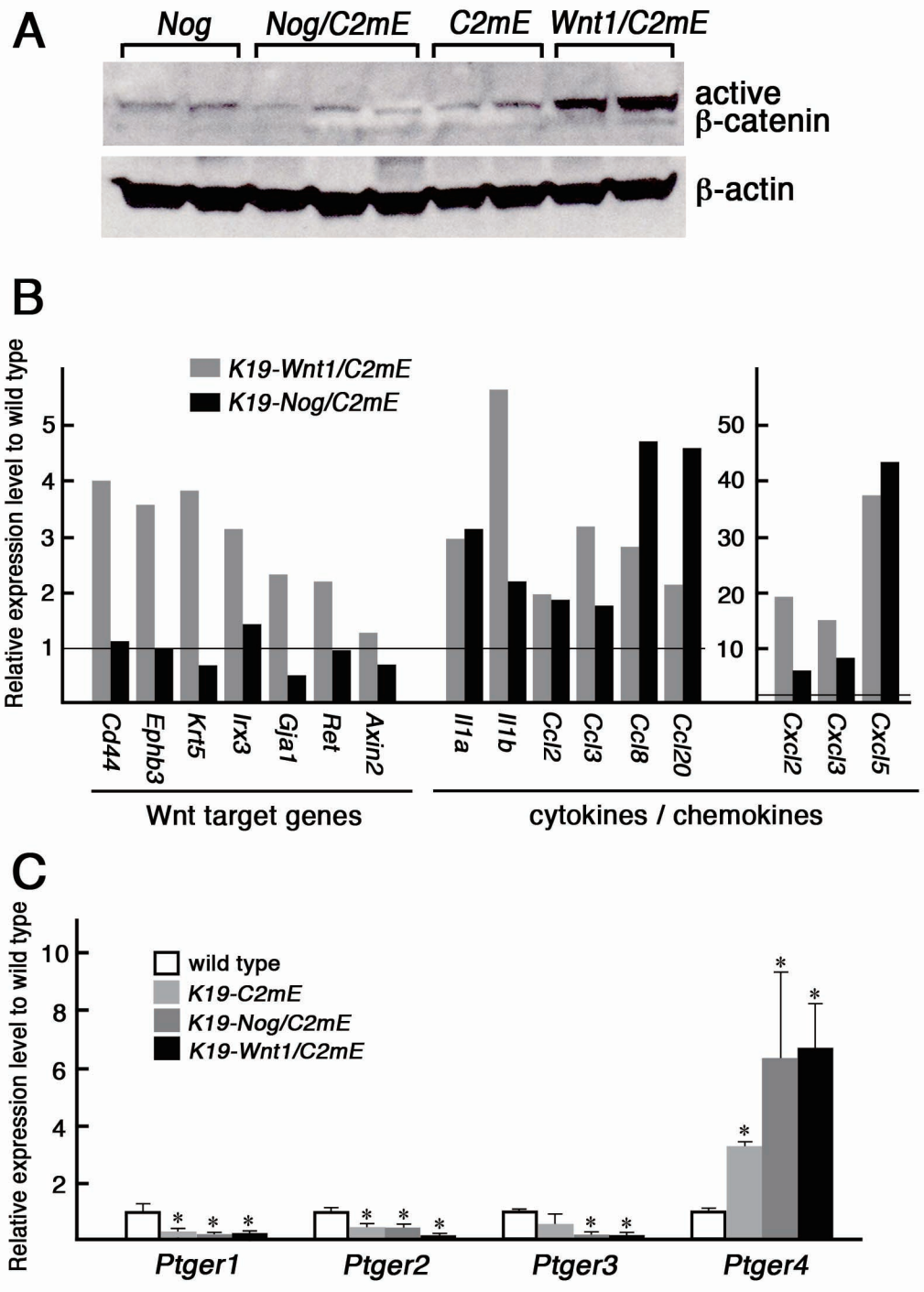
A
Nog
Nog/C2mE
C2mE
Wnt1/C2mE
active β-catenin
β-actin
B
Relative expression level to wild type
K19-Wnt1/C2mE
K19-Nog/C2mE
Cd44
Ephb3
Krt5
Irx3
Gja1
Ret
Axin2
Il1a
Il1b
Ccl2
Ccl3
Ccl8
Ccl20
Cxcl2
Cxcl3
Cxcl5
Wnt target genes
cytokines / chemokines
C
Relative expression level to wild type
wild type
K19-C2mE
K19-Nog/C2mE
K19-Wnt1/C2mE
Ptger1
Ptger2
Ptger3
Ptger4